

Important Notice to Authors

Physical Review B has recently changed its composition service provider, effective with the first issue of volume 83 (January 2011). You will note that the cover letter accompanying your proofs, as well as instructions on how to return proof corrections, are somewhat different than in the past. We thank you for your patience during the transition period and regret any inconvenience this may cause.

Attached is a proof copy of your forthcoming article in *Physical Review B*. The Article ID is **BE12007**.

To print the pdf proof full size, be sure that you have not selected the “fit to page” option.

Your paper will be in the following section of the journal: Articles

Figures submitted electronically as separate PostScript files containing color usually appear in color in the online journal. However, all figures will appear in the print journal in black and white if you have not requested color-in-print reproduction and paid the applicable charges for color figures. For figures that will be color online but grayscale in print, please insure that the text and caption clearly describe the figure to readers who view it only in black and white.

No further publication processing will occur until we receive your response to this proof.

Questions and Comments to Address

Your article has 10 pages.

The numbered items below correspond to numbers in the margin of the proof pages pinpointing the source of the question and/or comment. The numbers will be removed from the margins prior to publication.

- 1 Please check change to “Im” in Eq. (12) and throughout.
- 2 Please check city for Ref. 8.
- 3 Please provide pg. no. for Ref. 18.
- 4 Please check Ref. 25.

Q: This reference could not be linked due to a possible error in any of the following: journal title, author name(s), volume, page, or year. Please check all information for accuracy and correct as necessary.

Other Items to Check

- Please check your title, author list, receipt date, and PACS numbers. More information on PACS numbers is available online at <http://publish.aps.org/PACS/>.
- Please proofread the article very carefully.
- Please check that your figures are accurate and sized properly. Figure quality in this proof is the quality to be used in the online journal. To achieve manageable file size for online delivery, some compression and downsampling of figures may have occurred. Fine details may have become somewhat fuzzy, especially in color figures. The print journal uses files of higher resolution and therefore details may be sharper in print. Figures to be published in color online will appear in color on these proofs if viewed on a color monitor or printed on color printer.

Ways to Respond

- **Web:** If you accessed this proof online, follow the instructions on the web page to submit corrections.
- **Email:** Send corrections
To: prbproofs@aptaracorp.com
Subject: **BE12007** proof corrections
- **Fax:** Return this proof with corrections to +1.703.352.8862. Write **Attention:** PRB Project Manager and the Article ID, **BE12007**, on the proof copy unless it is already printed on your proof printout.
- **Mail:** Return this proof with corrections to **Attention:** PRB Project Manager, Physical Review B, c/o Aptara, 3110 Fairview Park Drive, Suite #900, Falls Church, VA 22042-4534, USA.

Superconductivity in multiband disordered systems: A vector recursion approach

Shreemoyee Ganguly

Department of Materials Science, S.N. Bose National Centre for Basic Sciences, JD-III Salt Lake City, Kolkata 700098, India

Indra Dasgupta

Department of Solid State Physics and Centre for Advanced Materials, Indian Association for the Cultivation of Science, Jadavpur, Kolkata 700032, India

Abhijit Mookerjee

Department of Materials Science and Advanced Materials Research Unit, S.N. Bose National Centre for Basic Sciences, JD-III Salt Lake City, Kolkata 700098, India

(Received 26 May 2011; revised manuscript received 19 October 2011; published xxxxx)

We present a vector recursion based approach to study the effect of disorder on superconductivity in a system modeled by the two-band attractive Hubbard model. We use the augmented space formalism for the disorder averaging. In the presence of only intraband pairing in a two-band disordered system with disorder in either or both bands, our calculations reveal that the gap survives in the quasiparticle spectrum; similar to single band systems. However, for interband pairing the gap in the quasiparticle spectrum ceases to exist beyond a critical value of the disorder strength. In the presence of both interband and intraband pairing interaction, depending on the relative magnitude of the pairing strength, only a particular kind of pairing is possible for a half filled two-band system.

DOI: [10.1103/PhysRevB.00.004500](https://doi.org/10.1103/PhysRevB.00.004500)

PACS number(s): 71.10.-w, 71.23.-k, 74.20.-z

I. INTRODUCTION

The study of superconductivity in multiband systems has received considerable interest recently because of the discovery of superconducting materials where the Fermi surface is dominated by several bands. Examples include MgB_2 where the Fermi surface is determined by the σ and π bands arising from the $B-p$ orbitals. It is now confirmed that the superconductivity in this material can be explained with the Bardeen-Cooper-Schrieffer (BCS) theory with two different superconducting gaps in agreement with experiments.¹ A description of unusual p -wave superconductivity in Sr_2RuO_4 also necessitates a multiband model for superconductivity.^{2,3} Very recently the discovery of superconductivity in Fe pnictides, whose Fermi surface is built out of the t_{2g} orbitals of Fe, has again emphasized the importance of the study of superconductivity in multiband systems.^{4,5}

The complex problem of superconductivity in multiband systems was first studied by Suhl *et al.*⁶ using a tight-binding model Hamiltonian with two bands. The model included intraband pairing and also the interband hopping of pairs of electrons belonging to the same band. They showed that pairing could occur in each band and, because electron-phonon interactions may have different strengths in different bands, this can give rise to two different superconducting gaps. But in the special case of only interband scattering, a single gap was found to be present in the density of states unless the band dispersion of the two bands had different shapes.⁷ A similar model was also investigated by Machida *et al.*⁸ for the study of superconductivity in multiband systems. Recently Moreo *et al.*⁹ revisited the theory of superconductivity in multiband systems in the context of Fe pnictides. In particular they have emphasized the importance of interband pairing in multiband

systems in which, in contrast to earlier studies,^{6,8} Cooper pairs are formed by electrons belonging to two different bands. The calculations by Moreo *et al.*⁹ revealed that three different regions can result from a purely interband pairing as a function of the interaction parameter: (i) a normal regime where the ground state is not superconducting; (ii) an exotic superconducting “breached” regime where one of the bands is gapped at the Fermi level while the other is not, and (iii) a superconducting regime resembling the BCS states, at large attractive coupling. The existence of an exotic superconducting “breached” regime with both gapped and gapless quasiparticle excitations was also discussed by Liu and Wilczek¹⁰ in the context of cold atoms and quantum chromodynamic systems.

The preceding discussion suggests that superconductivity in multiband systems is not only interesting but markedly different from its single-band counterpart. In this context it will also be important to understand the role of disorder in multiband superconducting systems since disorder is an important factor that has a profound impact on superconductivity. While the effect of disorder on superconductivity in single-band systems have been actively investigated, there are very few systematic studies of the role of disorder in multiband systems.

The effect of disorder in single-band systems is usually discussed within the framework of Anderson’s theorem.¹¹ For s -wave superconductors Anderson’s theorem guarantees the survival of an absolute gap in the quasiparticle spectrum of the system provided the perturbation due to disorder preserves time-reversal invariance and the coherence length is long enough to ensure that the pairing amplitude Δ does not fluctuate. There exists a body of work where the Bogoliubov–de Gennes (BdG) equations,¹² which provide

87 a natural framework for a fully microscopic description
88 of the phenomena of superconductivity, have been solved
89 in conjunction with the mean-field single-site coherent po-
90 tential approximation (CPA),^{13–15} in order to understand
91 the physics of superconductivity in single-band disordered
92 systems.

93 Recently we have proposed an efficient real-space scheme
94 to solve the BdG equations for single-band disordered attrac-
95 tive Hubbard models.¹⁶ The aim of this paper is to propose
96 a real space, vector recursion based approach to study the
97 effect of disorder on a multiband attractive- U Hubbard model
98 where the configuration averaging, as in our earlier study, will
99 be based on the augmented space recursion (ASR) formalism
100 introduced by one of us.¹⁷ The ASR gives us the flexibility of
101 introducing the effects of random configuration fluctuations in
102 the local environment of a site. It does not violate analytical
103 properties of the configuration-averaged Green's function,
104 which form an essential ingredient of the solution. It can
105 deal easily with the effect of either off-diagonal disorder or
106 inhomogeneous disorder such as clustering, segregation, and
107 short-ranged ordering, which usually occur intrinsically in
108 most disordered materials due to different chemical affinities
109 of the constituents.

110 We shall begin by studying superconductivity in an or-
111 dered two-band, tight-binding, attractive- U Hubbard model,
112 using our vector recursion technique. Then, having satisfied
113 ourselves with the reliability of our methodology, we shall
114 proceed to study the effect of disorder on the same model.
115 The rest of the paper is organized as follows: in Sec. II we
116 shall discuss our method in some detail. Section III will be
117 devoted to results and discussions for multiband ordered and
118 disordered systems. Finally in Sec. IV we will summarize our
119 study.

120 II. METHODOLOGY

121 A. Multiband attractive- U Hubbard model

122 To study the effect of disorder on a multiband s -wave
123 superconducting system we shall begin with the simplest
124 model, namely, the two-band attractive Hubbard Hamiltonian
125 in model lattices. The Hamiltonian is given by

$$\begin{aligned} \mathbf{H} = & - \sum_{(i,j)} \sum_{m,m',\sigma} t_{im,jm'} c_{im\sigma}^\dagger c_{jm'\sigma} + \sum_{i,m,\sigma} (\varepsilon_{im} - \mu) n_{im\sigma} \\ & - \sum_{i,m} |U_{mm}(i)| n_{im\uparrow} n_{im\downarrow} \\ & - \sum_i \sum_{m,m',\sigma,\sigma'} |U_{mm'}(i)| n_{im\sigma} n_{im'\sigma'}. \end{aligned} \quad (1)$$

126 Here m, m' are the band index. This Hamiltonian is a
127 generalization of the single-band Hubbard Hamiltonian and

is similar to earlier studies by Annett and co-workers.^{3,18} 128
Our model Hamiltonian allows for both intraband as well as 129
interband pairing. The interband pairing term is similar to 130
that of Annett and co-workers^{3,18} and Moreo *et al.*⁹ which 131
allows Cooper pairs to be formed by electrons belonging 132
to two different bands. The earlier studies by Suhl *et al.*⁶ 133
and Machida *et al.*⁸ did not consider the pairing of electrons 134
belonging to two different bands but a pair tunneling term 135
given by 136

$$- \sum_i \sum_{m,m',\sigma,\sigma'} |U_{mm'}^t(i)| (c_{im\sigma} c_{im'\sigma'})^\dagger c_{im'\sigma} c_{im\sigma}. \quad (2)$$

This term allowed for the tunneling of the Cooper pairs from 137
one band to the other with a tunneling strength given by 138
 $U_{mm'}^t$. 139

In Eq. (1) $\{c_{im\sigma}^\dagger\}, \{c_{im\sigma}\}$ are the usual electron creation and 140
annihilation operators for orbital m with spin σ on site labeled 141
 i of a square or cubic lattice. The index m runs over the two 142
bands labeled s and l , μ is the chemical potential, and ε_{im} 143
is the local on-site energy at the site labeled i in the band m . The 144
hopping integral $t_{im,jm'}$ has four components: $t_{is,js} = t_s$ is the 145
hopping integral in the s band from a site i to one of its nearest 146
neighbors j and $t_{il,jl} = t_l$ is that in the l band from a site to 147
one of its nearest neighbors. The interband hopping integrals 148
are $t_{is,il} = t_{sl}$, which is the hopping integral from a site in 149
the s band to the same site in the l band (or vice versa) and 150
 $t_{is,jl} = t_{sl}^{nn}$, which is the hopping integral from a site i in the 151
 s band to one of its nearest neighbors j in the l band (or vice 152
versa). In this work we have not included the interband intersite 153
hopping integral t_{sl}^{nn} . However, we do consider the effect of 154
on-site interband hopping integrals t_{sl} in some of our analysis. 155
As we will see subsequently, t_{sl} will not alter the qualitative 156
features of our results. In this model, $U_{ss} = -|U_s|$ corresponds 157
to a local Hubbard parameter leading to a pairing interaction 158
potential for s -band electrons and $U_{ll} = -|U_l|$ correspond to 159
a local Hubbard parameter for l -band electrons. Here, both the 160
attractive interactions give rise to s -wave pairing since they 161
are local. The interband pairing interaction $U_{mm'} = -|U_{sl}|$ is 162
the local attractive potential between electrons in the s and l 163
band. 164

The BdG mean-field decomposition¹² of the interaction 165
terms give expectation values to the intra- and interband pairing 166
amplitudes, 167

$$\Delta_m = -|U_m| \langle c_{im\downarrow} c_{im\uparrow} \rangle; \quad \Delta_{sl} = -|U_{sl}| \langle c_{il\downarrow} c_{is\uparrow} \rangle, \quad (3)$$

and also to the intra- and interband “densities,” 168

$$\langle n_{im\sigma} \rangle = \langle c_{im\sigma} c_{im\sigma}^\dagger \rangle; \quad \langle n_{isl\sigma} \rangle = \langle c_{il\sigma} c_{is\sigma}^\dagger \rangle. \quad (4)$$

The effective quadratic BdG Hamiltonian becomes 169

$$\begin{aligned} \mathbf{H}_{\text{eff}} = & - \sum_{(i,j)} \sum_{m,m',\sigma} t_{im,jm'} c_{im\sigma}^\dagger c_{jm'\sigma} + \sum_{im\sigma} (\varepsilon_{im} - \hat{\mu}_{im}) n_{im\sigma} - \sum_{im,m',\sigma} |U_{mm'}| \frac{\langle n_{imm'\sigma} \rangle}{2} c_{im\sigma}^\dagger c_{jm'\sigma} \\ & + \sum_{im} (\Delta_m c_{im\uparrow}^\dagger c_{im\downarrow}^\dagger - \Delta_m^* c_{im\uparrow} c_{im\downarrow}) + \sum_{i,m,m'} (\Delta_{mm'} c_{im\uparrow}^\dagger c_{im'\downarrow}^\dagger - \Delta_{mm'}^* c_{im\uparrow} c_{im'\downarrow}), \end{aligned} \quad (5)$$

170 where $\hat{\mu}_{im} = \mu - |U_{mm}| \langle n_{im} \rangle / 2$ incorporates the site dependent Hartree shift.

172 This effective Hamiltonian can be diagonalized by using the Hartree-Fock-Bogoliubov (HFB)¹⁹ transformation,

$$\begin{aligned} c_{im\uparrow} &= \sum_n [\beta_{n\uparrow} u_m(r_i, E) - \beta_{n\downarrow}^{\dagger} v_m^*(r_i, E)], \\ c_{im\downarrow} &= \sum_n [\beta_{n\downarrow} u_m(r_i, E) + \beta_{n\uparrow}^{\dagger} v_m^*(r_i, E)], \end{aligned} \quad (6)$$

174 where β and β^{\dagger} are quasiparticle operators, and $u_m(r_i, E)$, $v_m(r_i, E)$ are the quasiparticle amplitudes associated with an eigenenergy E_n .

177 In the Hartree-Fock mean-field approximation incorporating charge-order and superconducting decoupling along with the above canonical transformation we have

$$\begin{aligned} &\begin{pmatrix} H_{ss} & \Delta_s & -N_{sl} & \Delta_{sl} \\ \Delta_s^* & -H_{ss} & \Delta_{sl}^* & N_{sl} \\ -N_{ls} & \Delta_{ls} & H_{ll} & \Delta_l \\ \Delta_{ls}^* & -N_{ls} & \Delta_l^* & -H_{ll} \end{pmatrix} \begin{pmatrix} u_s(r_i, E) \\ v_s(r_i, E) \\ u_l(r_i, E) \\ v_l(r_i, E) \end{pmatrix} \\ &= E \begin{pmatrix} u_s(r_i, E) \\ v_s(r_i, E) \\ u_l(r_i, E) \\ v_l(r_i, E) \end{pmatrix}, \end{aligned} \quad (7)$$

180 where (the excitation eigenvalue $E \geq 0$)

$$\begin{aligned} H_{mm} u_m(r_i, E) &= (\varepsilon_m - \hat{\mu}_{im}) u_m(r_i, E) - \sum_j t_{mj} u_m(r_j, E), \\ N_{mm'} u_{m'}(r_i, E) &= \left\{ \frac{1}{2} |U_{mm'}| \langle n_{mm'} \rangle + t_{mm'} \right\} u_{m'}(r_i, E) \\ &+ \sum_j t_{mm'}^{nn'} u_{m'}(r_j, E). \end{aligned} \quad (8)$$

181 Here j is the nearest neighbor of i . We can express the particle densities and the pairing amplitudes in terms of the quasiparticle amplitude as

$$\begin{aligned} \langle n_{im} \rangle &= 2 \int dE |u_m(r_i, E)|^2 f(E) \\ &+ |v_m(r_i, E)|^2 [1 - f(E)], \\ \langle n_{imm'} \rangle &= 2 \int dE u_{m'}(r_i, E) u_m^*(r_i, E) f(E) \\ &+ v_m^*(r_i, E) v_{m'}(r_i, E) [1 - f(E)], \\ \Delta_m &= |U_m| \int dE v_m^*(r_i, E) u_m(r_i, E) f(E) \\ &- u_m(r_i, E) v_m^*(r_i, E) [1 - f(E)], \\ \Delta_{mm'} &= |U_{mm'}| \int dE v_m^*(r_i, E) u_{m'}(r_i, E) f(E) \\ &- u_m(r_i, E) v_{m'}^*(r_i, E) [1 - f(E)], \end{aligned} \quad (9)$$

184 where $f(E)$ is the Fermi function. A fully self-consistent solution of Eq. (7) can be obtained provided all the normal potentials ($|U_m| \langle n_{im} \rangle$ and $|U_{mm'}| \langle n_{imm'} \rangle$) and anomalous potentials (Δ_{im} and $\Delta_{imm'}$) are determined self-consistently from Eq. (9). The self-consistency criteria is set to 10^{-6} for calculation of all self-consistent parameters throughout the present study.

B. Treatment of disorder: Augmented space formalism

The class of systems which we shall study here will be binary substitutionally disordered alloys. We shall study randomness in the diagonal site energies, either in one of the two bands, say the l band ($\{\varepsilon_{il}\}$); or in both the bands ($\{\varepsilon_{is}\}$ and $\{\varepsilon_{il}\}$). We shall introduce site occupation variables $\{n_i\}$ (this should not be confused with the number operator $n_{im\sigma}$) which take values 1 or 0 according to whether the site labeled i is occupied by an A type or a B type of atom,

$$\varepsilon_{im} = \varepsilon_m^A n_i + \varepsilon_m^B (1 - n_i) = \varepsilon_m^B + \delta\varepsilon_m n_i, \quad (10)$$

where, $m = s$ or l and ε_s^A , ε_s^B and ε_l^A , ε_l^B are the possible on-site energies corresponding to the s and l band, respectively. We define the strength of disorder in the band labeled m by $D_m = |\delta\varepsilon_m| = |\varepsilon_m^A - \varepsilon_m^B|$.

If the concentrations of A - and B -type atoms in the solid are x and y , then the probability density of n_i , in the absence of short-range order, is given by

$$p(n_i) = x\delta(n_i - 1) + y\delta(n_i). \quad (11)$$

The ‘‘configuration space’’ of n_i , Φ_i , has rank 2 and is spanned by the states $|A_i\rangle$ and $|B_i\rangle$ in which the parameter ε_{im} take the values ε_m^A and ε_m^B , respectively.

The augmented space formalism associates with each random variable n_i an operator \tilde{N}_i acting on its configuration space Φ_i and whose spectral density is its probability density. That is,

$$p(n_i) = -\frac{1}{\pi} \lim_{\delta \rightarrow 0} \text{Im} \langle \emptyset_i | [(n_i + i\delta)\tilde{I} - \tilde{N}_i]^{-1} | \emptyset_i \rangle, \quad (12)$$

where $|\emptyset_i\rangle = \sqrt{x}|A_i\rangle + \sqrt{y}|B_i\rangle$ is the so-called ‘‘reference’’ state. This nomenclature arises from the fact that the augmented space theorem²⁰ states that the matrix element in this state is the configuration average. The other basis member is $|1_i\rangle = \sqrt{y}|A_i\rangle - \sqrt{x}|B_i\rangle$ which is a state with one ‘‘fluctuation’’ about the reference state at the site i . Alternatively, it is denoted by $\{|i\rangle\}$ where $\{i\}$ is the ‘‘cardinality sequence’’ of sites at which there are fluctuations. The configuration states $|A_i\rangle$ and $|B_i\rangle$ are the eigenkets of \tilde{N}_i corresponding to eigenvalues 1 and 0. The representation of the operator \tilde{N}_i in the basis $\{|\emptyset_i\rangle, |1_i\rangle\}$ is

$$\begin{aligned} \tilde{N}_i &= xP_{\emptyset_i} + yP_{1_i} + \sqrt{xy}[T_{\emptyset_i, 1_i} + T_{1_i, \emptyset_i}] \\ &= xI + (y - x)P_{1_i} + \sqrt{xy}[T_{\emptyset_i, 1_i} + T_{1_i, \emptyset_i}]. \end{aligned} \quad (13)$$

Here, I is the identity operator, P_X are the projection operators $|X\rangle\langle X|$, and T_{XY} are the transfer operators $|X\rangle\langle Y|$, and X, Y are either \emptyset_i or 1_i .

Let us define a configuration fluctuation creation operator at the site labeled i as $\gamma_i^{\dagger} |\emptyset_i\rangle = |1_i\rangle$. Since each site can either be \emptyset or 1, this is a fermionlike creation operator with $\gamma_i^{\dagger} |1_i\rangle = 0$. Similarly we define a configuration fluctuation annihilation operator $\gamma_i |1_i\rangle = |\emptyset_i\rangle$ and $\gamma_i |\emptyset_i\rangle = 0$. In terms of these operators $P_{1_i} = \gamma_i^{\dagger} \gamma_i$ counts the number of configuration fluctuations at the site i , and of the transfer operators: $T_{\emptyset_i, 1_i} = \gamma_i$ annihilates and $T_{1_i, \emptyset_i} = \gamma_i^{\dagger}$ creates a configuration fluctuation at the site i .

The operator \tilde{N}_i in this new representation is

$$\tilde{N}_i = xI + (y - x)\gamma_i^{\dagger} \gamma_i + \sqrt{xy}(\gamma_i^{\dagger} + \gamma_i) \quad (14)$$

237 So,

$$\begin{aligned} \varepsilon_{im} &= \varepsilon_m^B + \delta\varepsilon_m n_i \quad \text{has associated with it an operator,} \\ \tilde{\varepsilon}_{im} &= \langle \varepsilon_m \rangle I + (y-x)\delta\varepsilon_m \gamma_i^\dagger \gamma_i + \sqrt{xy} \delta\varepsilon_m (\gamma_i^\dagger + \gamma_i) \end{aligned} \quad (15)$$

238 obtained by replacing n_i with its operator form \tilde{N}_i [see
239 Eq. (14)] where $\langle \varepsilon_m \rangle$ refers to the average:

$$\langle \varepsilon_m \rangle = x\varepsilon_m^A + y\varepsilon_m^B \quad (16)$$

240 with $m = s$ or l , $\delta\varepsilon_s = \varepsilon_s^A - \varepsilon_s^B$, and $D_s = |\delta\varepsilon_s|$, $\delta\varepsilon_l = \varepsilon_l^A -$
241 ε_l^B , and $D_l = |\delta\varepsilon_l|$.

242 The augmented space theorem²⁰ states that the configura-
243 tion average of a function of a set of independent random
244 variables $\mathbf{A}(\{n_i\})$ can be expressed as a matrix element
245 in the full configuration space of the disordered system

$$\begin{aligned} \tilde{\mathbf{H}}_{\text{eff}} &= - \sum_{(i,j),m,m',\sigma} t_{im,jm'} c_{im\sigma}^\dagger c_{jm'\sigma} \otimes I + \sum_{im\sigma} (\langle \varepsilon_m \rangle - \hat{\mu}_{im}) n_{im\sigma} \otimes I + \sum_{im\sigma} \delta\varepsilon_m n_{im\sigma} \otimes \{(y-x)\gamma_i^\dagger \gamma_i + \sqrt{xy}(\gamma_i^\dagger + \gamma_i)\} \cdots \\ &- \sum_{im,m',\sigma} |U_{mm'}| \frac{\langle n_{imm'\sigma} \rangle}{2} c_{im\sigma}^\dagger c_{jm'\sigma} \otimes I + \sum_{im} (\Delta_m c_{im\uparrow}^\dagger c_{im\downarrow}^\dagger - \Delta_m^* c_{im\uparrow} c_{im\downarrow}) \otimes I \cdots \\ &+ \sum_{i,m,m'} (\Delta_{mm'} c_{im\uparrow}^\dagger c_{im'\downarrow}^\dagger - \Delta_{mm'}^* c_{im\uparrow} c_{im'\downarrow}) \otimes I. \end{aligned} \quad (18)$$

260 In the special case when there is randomness in just one of the
261 bands (say l), in Eq. (18) we put $\delta\varepsilon_s = 0$ and $\langle \varepsilon_s \rangle = \varepsilon_s$.

262 After constructing the Hamiltonian in augmented space the
263 augmented space theorem then automatically ensures that the
264 configuration average is a projection onto the state with no
265 “fluctuations,”²⁰

$$\langle \langle \underline{\mathbf{G}}(i,i,E) \rangle \rangle = \langle \emptyset | \underline{\mathbf{G}}(i,i,E) | \emptyset \rangle,$$

266 where $\underline{\mathbf{G}} = (E\underline{\mathbf{I}} - \underline{\mathbf{H}}_{\text{eff}})^{-1}$. All operators here are 4×4 ma-
267 trices (here double underbar indicates 4×4 matrices) in the
268 space spanned by the two bands and the electron-hole degrees
269 of freedom²¹ arising in BdG formalism.

270 The Green’s functions are obtained using the vector
271 recursion technique introduced by Haydock and Godin.^{22,23}
272 The vector recursion has been described in great detail in the
273 given references and in our earlier work.¹⁶ We shall indicate
274 the main points and the interested reader may refer to the
275 quoted references for details. Once the BdG Hamiltonian
276 is set up as in Eq. (7) and the effective augmented space
277 transformation carried out as in Eq. (18), the vector recursion
278 technique essentially changes the basis in order to block tri-
279 diagonalize the effective Hamiltonian. The basis is recursively
280 generated,

$$\begin{aligned} |1\rangle &= \begin{pmatrix} u_s(\vec{r}_i, E) \otimes \{\emptyset\} \\ v_s(\vec{r}_i, E) \otimes \{\emptyset\} \\ u_l(\vec{r}_i, E) \otimes \{\emptyset\} \\ v_l(\vec{r}_i, E) \otimes \{\emptyset\} \end{pmatrix} \\ \underline{\underline{\mathbf{H}}}_{n+1} |n+1\rangle &= \underline{\underline{\mathbf{H}}}_n |n\rangle - \underline{\underline{\mathbf{A}}}_n |n\rangle - \underline{\underline{\mathbf{B}}}_n |n-1\rangle. \end{aligned}$$

$$\Phi = \prod_i^\otimes \Phi_i, \quad 246$$

$$\langle \langle \mathbf{A}(\{n_i\}) \rangle \rangle = \langle \{\emptyset\} | \tilde{\mathbf{A}}(\{\tilde{N}_i\}) | \{\emptyset\} \rangle, \quad (17)$$

247 where $|\{\emptyset\}\rangle = \prod_i^\otimes |\emptyset_i\rangle$ and $\tilde{\mathbf{A}}(\{\tilde{N}_i\})$ is the representation of
248 the operator $\tilde{\mathbf{A}}$ in the configuration space Φ , constructed by
249 replacing all random variables n_i by their corresponding
250 operators \tilde{N}_i . A compact way of representing a basis in
251 configuration space is to denote it by the set of sites where
252 we have a configuration fluctuation. This set is called the
253 *cardinality set* and the meaning of the empty cardinality
254 set $\{\emptyset\}$ then becomes obvious. For the present system the
255 Hamiltonian contains the random variables $\{\varepsilon_{is}\}$ and $\{\varepsilon_{il}\}$. So
256 we need to construct the Hamiltonian in the augmented space
257 $\Psi = \mathcal{H} \otimes \prod_i^\otimes \Phi_i$ by replacing all the random variables ε_{is}
258 and ε_{il} by the corresponding operators shown in Eq. (15). The
259 effective augmented space Hamiltonian becomes

281 The coefficients $\underline{\underline{\mathbf{A}}}_n$ and $\underline{\underline{\mathbf{B}}}_n$ are matrices and obtained from
282 the orthogonality of the generated basis and between rows
283 of the same basis. The configuration averaged diagonal matrix
284 element of the Green’s function then follows as a matrix
285 continued fraction,

$$\langle \langle \underline{\underline{\mathbf{G}}}(\vec{r}_i, \vec{r}_i; E) \rangle \rangle = \langle \langle 1 | \underline{\underline{\mathbf{G}}} | 1 \rangle \rangle = \underline{\underline{\mathbf{G}}}_0(E),$$

$$\underline{\underline{\mathbf{G}}}_n(E) = [z\underline{\underline{\mathbf{I}}} - \underline{\underline{\mathbf{A}}}_n - \underline{\underline{\mathbf{B}}}_{n+1}^\dagger \underline{\underline{\mathbf{G}}}_{n+1}(E) \underline{\underline{\mathbf{B}}}_{n+1}]^{-P_n-1},$$

$$n = 0, 1, 2, \dots, N_2 - 1,$$

286 where A^{-P_n} denotes inverse in the subspace spanned by the
287 basis $\{|n+1\rangle, |n+2\rangle, \dots\}$. The matrix continued fraction is
288 terminated in two steps. The matrix coefficients $\{\underline{\underline{\mathbf{A}}}_n, \underline{\underline{\mathbf{B}}}_n\}$ are
289 calculated exactly for $n < N_1$, then: first, by putting $\underline{\underline{\mathbf{A}}}_n = \underline{\underline{\mathbf{A}}}_{N_1}$
290 and $\underline{\underline{\mathbf{B}}}_n = \underline{\underline{\mathbf{B}}}_{N_1}$ for all $N_1 \leq n < N_2$ and second, $\underline{\underline{\mathbf{G}}}_{N_2}(E) =$
291 $(E + i\eta)^{-1} \underline{\underline{\mathbf{I}}}$.

292 The physical quantities of interest [Eq. (9)] relevant to the
293 study can be expressed as appropriate matrix elements of the
294 Green’s function,

$$\begin{aligned} \langle n_m \rangle &= -\frac{1}{\pi} \lim_{\eta \rightarrow 0} \text{Im} \int_{-\infty}^{\infty} [\mathbf{G}_{mm}^{++}(i, i, E + i\eta) f_n \\ &+ \mathbf{G}_{mm}^{--}(i, i, E + i\eta) (1 - f_n)] dE, \\ \Delta_m &= -\frac{1}{\pi} \lim_{\eta \rightarrow 0} \text{Im} \int_{-E_c}^{+E_c} [\mathbf{G}_{mm}^{+-}(i, i, E + i\eta) f_n \\ &+ \mathbf{G}_{mm}^{-+}(i, i, E + i\eta) (1 - f_n)] dE, \end{aligned}$$

$$\begin{aligned}
\langle n_{mm'} \rangle &= -\frac{1}{\pi} \lim_{\eta \rightarrow 0} \text{Im} \int_{-\infty}^{\infty} [\mathbf{G}_{mm'}^{++}(i, i, E + i\eta) f_n \\
&\quad + \mathbf{G}_{mm'}^{--}(i, i, E + i\eta)(1 - f_n)] dE, \\
\Delta_{mm'} &= -\frac{1}{\pi} \lim_{\eta \rightarrow 0} \text{Im} \int_{-E_c}^{+E_c} [\mathbf{G}_{mm'}^{+-}(i, i, E + i\eta) f_n \\
&\quad + \mathbf{G}_{mm'}^{-+}(i, i, E + i\eta)(1 - f_n)] dE, \quad (19)
\end{aligned}$$

295 where + and - refer to electron and hole spaces of the BdG
296 formalism²¹ and the energy interval $[-E_c, +E_c]$ is the short
297 interval around the Fermi energy of the system where the
298 interaction has its effect.

299 III. RESULTS AND DISCUSSION

300 A. Ordered systems

301 In this section we shall present results on ordered two-band
302 superconductors (both the bands having s -orbital character)
303 on square and cubic lattices with both local intra- and
304 interband Hubbard parameters. The system is kept fixed at
305 half filling unless otherwise stated. Since these results are well
306 known from other approaches, a comparison with them will
307 ascertain the viability and numerical accuracy of our proposed
308 methodology.

309 For our model system the hopping integrals are chosen
310 as follows: in Figs. 1(a)–1(d) the intraband nearest-neighbor
311 hopping elements are $t_s = 1.0$ and $t_l = 0.5$ and the interband
312 on-site hopping is $t_{sl} = 0.0$.

313 The s - and l -band partial densities of states (PDOS) for
314 the case when $U_s = U_l = U_{sl} = 0$ for the ordered system
315 are shown in Figs. 1(a) and 1(c) for the square and cubic
316 lattices, respectively. The two sets of PDOS exactly match
317 the standard calculations using Bloch's theorem. One can
318 clearly see in Fig. 1(a) the band-center integrable Van Hove
319 singularity, the two flanking kink singularities, and the square-
320 root singularities at the band edges that are characteristic of
321 a square lattice. The cubic lattice PDOS [see Fig. 1(c)] is
322 characterized by constant DOS at the band center and terminate
323 in kink singularities on both sides. The s band with greater
324 intraband hopping integral is wider, as expected.

325 Next we investigate the situation in the presence of
326 intraband pairing, i.e., Hubbard parameter U_s and U_l are only
327 finite. This corresponds to the system studied by Suhl *et al.*⁶
328 in the absence of interband tunneling of electrons. Thus U_{sl}
329 in Eq. (1) is set to zero. In Figs. 1(b) and 1(d) we consider
330 the cases where $U_s = U_l = 4.0$ and the system is kept fixed
331 at half filling. The BdG equations are solved recursively and
332 self-consistently as described earlier. After self-consistency
333 the superconducting order parameters Δ_s and Δ_l are found to
334 be nonzero. The s and l configuration averaged PDOS for the
335 system are calculated by using the relation

$$\langle \langle n_m(E) \rangle \rangle = -\frac{1}{\pi} \lim_{\eta \rightarrow 0} \text{Im} \langle \langle G_{mm}^{++}(1, 1, E + i\eta) \rangle \rangle,$$

336 where $m = s$ or l , η is an infinitesimal positive imaginary part
337 of the energy, and + refer to the electron states in the BdG
338 formalism.

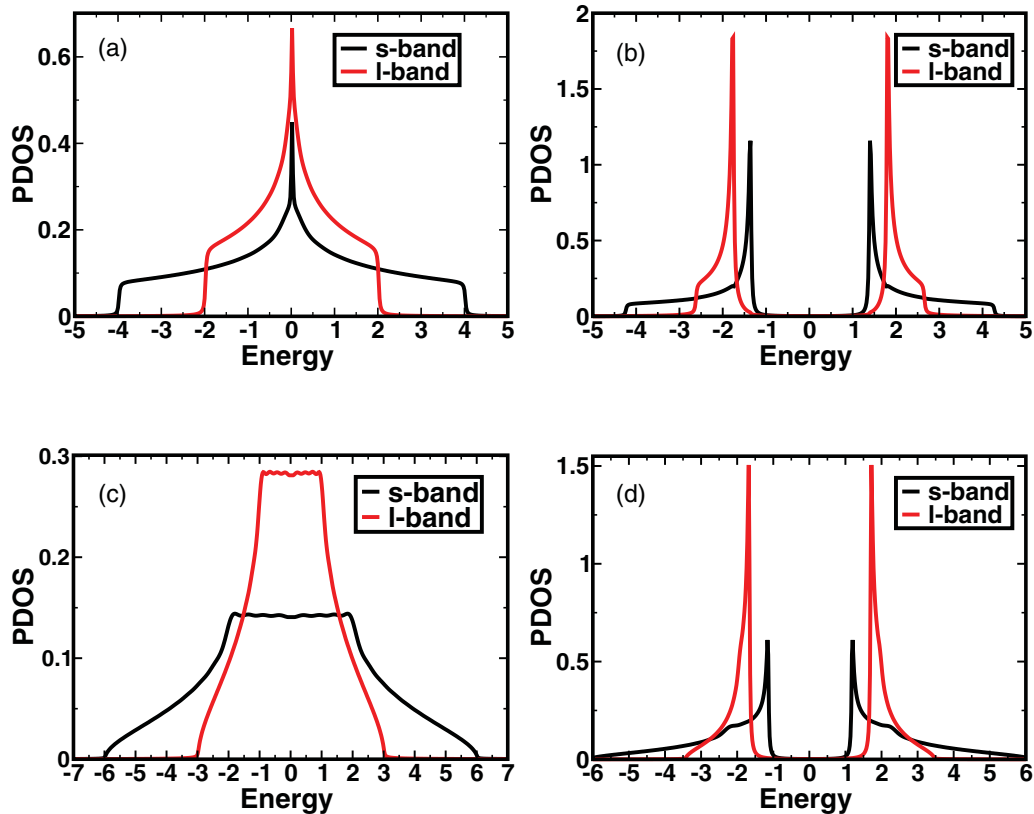


FIG. 1. (Color online) Study of superconductivity in an ordered square lattice [(a) and (b)] and cubic lattice [(c) and (d)] having two bands s and l . (1) Intraband hopping integrals $t_s = 1.0$ and $t_l = 0.5$, and (2) Hubbard parameters for (a) and (c) are $U_s = U_l = U_{sl} = 0.0$ and for (b) and (d) are $U_s = U_l = 4.0$ and $U_{sl} = 0.0$.

339 The PDOS shown in Figs. 1(b) and 1(d) reveal that in
 340 spite of the parameters $U_s = U_l$, the superconducting pairing
 341 amplitude Δ_s and Δ_l are different. This is due to the difference
 342 in bandwidth (W) as $t_s \neq t_l$, and the observation that the
 343 effective parameters U_m/W ($m = s$ or l) are responsible for
 344 the magnitude of the gap seen in the local DOS.

345 In view of the above we have also investigated the situation
 346 only with intraband Hubbard parameters such that $U_s \neq U_l$.
 347 We have considered $U_s = 3.0$ and $U_l = 1.0$. Since the effective
 348 parameter $U_s/W = 0.75 > U_l/W = 0.5$ we did find $\Delta_s > \Delta_l$.
 349 The earlier study by Suhl *et al.*⁶ had also found two different
 350 band gaps arising in a two-band model system. Two different
 351 superconducting gaps were later realized in MgB₂.²⁴⁻³⁰

352 Next in addition to the intraband pairing we have also
 353 included interband pairing of electrons. In the presence of
 354 both inter- and intraband Hubbard parameters an interesting
 355 competitive effect sets in, as can be seen from Fig. 2(a).
 356 We keep the intraband attractive Hubbard parameter fixed
 357 ($U_s = U_l = 2.0$), and vary the interband Hubbard parameter
 358 U_{sl} . The intraband hopping integrals are chosen to be $t_s = 1.0$
 359 and $t_l = 0.5$ and interband on-site hopping integral is $t_{sl} = 0.2$.
 360 We see [from Fig. 2(a)] when $U_s = U_l \geq U_{sl}$ then it is the
 361 intraband pairing amplitude that is only finite and the interband
 362 pairing amplitude vanishes. On the other hand, when $U_s =$
 363 $U_l < U_{sl}$ then it is only the interband pairing amplitude that is
 364 nonzero. Our calculations shows for momentum independent
 365 pairing in s -like bands depending on the strength of the
 366 attractive interaction, only a particular kind of pairing, either
 367 intraband or interband, is possible for two-band half filled
 368 systems when both bands have s -wave character.

369 Finally, we examine the effect of the interband (on-site)
 370 hopping integral t_{sl} on the pairing amplitude Δ for a half filled
 371 system. Figures 2(b) and 2(c) display the case for dominant
 372 intraband pairing ($U_s = U_l = 3.5 > U_{sl} = 2.0$) and dominant
 373 interband pairing ($U_s = U_l = 2.0 < U_{sl} = 3.5$), respectively.
 374 We find from the figures that inclusion of intraband on-site
 375 hopping term t_{sl} does not change the qualitative picture for a
 376 two-band system except to reduce the magnitude of the gap.

377 B. Homogeneously disordered systems

378 We shall now study an attractive- U Hubbard model of a
 379 two-band, disordered, binary substitutional alloy on a square
 380 lattice. First we consider randomness in the on-site energy in
 381 one of the two channels, namely the l channel, and study its
 382 effect on the other channel. We introduce randomness in the
 383 on-site energy using Eq. (15) and our Hamiltonian takes the
 384 form given in Eq. (18). The concentrations are $x = y = 0.5$
 385 and the system is half filled throughout the study.

386 To begin with, we study the systems in a situation similar
 387 to those under which we had investigated the corresponding
 388 ordered system. We keep $t_s = 1.0$ and $t_l = 0.5$ and the
 389 strength of disorder $D_l = |\varepsilon_l^A - \varepsilon_l^B| = 1$ throughout the cases
 390 considered in Fig. 3.

391 First we study the case when the system is nonsupercon-
 392 ducting ($U_s = U_l = U_{sl} = 0.0$). From Fig. 3(a) we find due
 393 to the absence of hybridization between the s and l bands
 394 the s PDOS is not affected by randomness in the l channel.
 395 The l PDOS [Fig. 3(b)], however, has characteristic features of
 396 disordered DOS: namely increase in bandwidth and smoothing

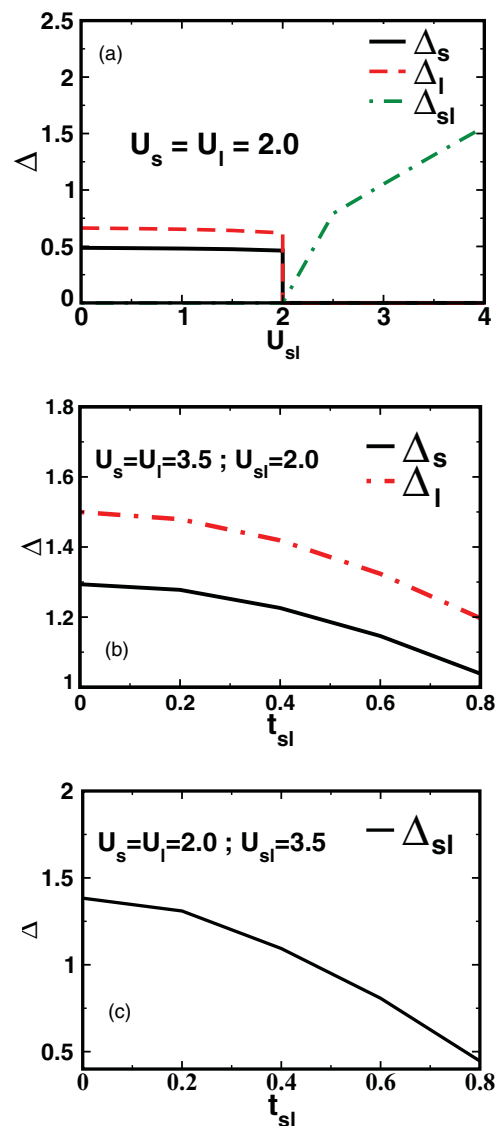


FIG. 2. (Color online) Variation of Δ for a square lattice when both intra- and interband interaction potentials are nonzero. Here the intraband hopping integrals are $t_s = 1.0$ and $t_l = 0.5$ for the s and l bands, respectively. In (a) the intraband pairing potentials $|U_s|$ and $|U_l|$ are kept fixed at 2.0 and U_{sl} is varied. In (b) and (c) the pairing potentials are kept fixed [(b) $U_s = U_l > U_{sl} = 2.0$ and (c) $U_s = U_l < U_{sl} = 3.5$] and the effect of variation of interband on-site hopping integral t_{sl} is studied.

397 out of Van Hove singularities. The total DOS [Fig. 3(c)]
 398 therefore carries the signatures of disorder as well.

399 Next, we investigate the DOS of the same system consider-
 400 ing only the intraband Hubbard parameters to be nonzero, i.e.,
 401 $U_s = U_l = 4.0$ and $U_{sl} = 0.0$ [Figs. 3(d)–3(f)]. In this case
 402 only the intraband pairing amplitudes Δ_s and Δ_l are nonzero
 403 [see Eq. (3)]. We see that the s PDOS remains unaffected
 404 by randomness in the l channel [comparing Fig. 3(d) with
 405 Fig. 1(b)], disorder, however, influences the l PDOS [comparing
 406 Fig. 3(e) with Fig. 1(b)]. Since both the s PDOS and l PDOS
 407 are gapped, the total DOS remains gapped [Fig. 3(f)]. Similar
 408 behavior also prevails with the inclusion of attractive interband

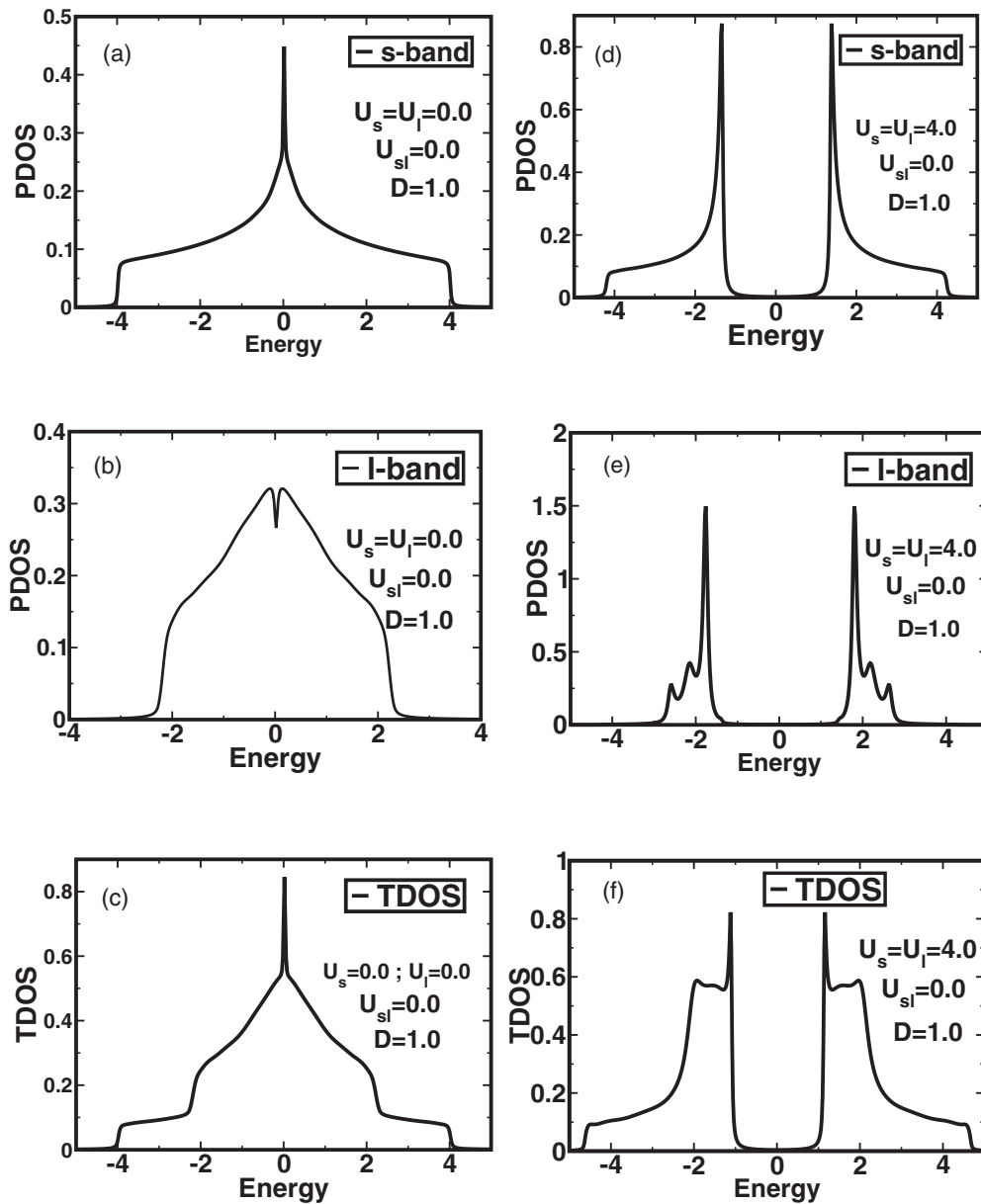


FIG. 3. Study of a two-band superconducting system in a square lattice with disorder in the l channel with strength of disorder $D = 1.0$. While (a)–(c) study the s , l PDOS and total DOS, respectively, for the nonsuperconducting case (where intra- and interband Hubbard potential $U_s = U_l = U_{sl} = 0.0$), (d)–(f) study the effect of disorder on the corresponding superconducting system with only intraband interaction.

409 interaction U_{sl} , provided the intraband pairing dominates, i.e.,
 410 $U_{sl} < U_l$ and U_s .

411 The variation of the zero-temperature superconducting
 412 order parameters Δ_s , Δ_l , and Δ_{sl} are plotted as a function of
 413 the strength of disorder in Fig. 4(a) where $U_s = U_l = 2.0 >$
 414 $U_{sl} = 1.0$. As expected for momentum independent pairing
 415 only the intraband pairings are finite. Δ_s does not change as a
 416 function of disorder strength as it does not register the effect
 417 of the disorder in the l channel. As the strength of disorder
 418 (D) is increased Δ_l reduces but remains finite even for $D = 3$.
 419 Therefore in the chosen parameter regime for the two-band
 420 system the situation is similar to that predicted by Anderson
 421 theorem¹¹ for the single-band system, where the gap survives
 422 in the quasiparticle spectrum even in the presence of disorder.

423 Suhl *et al.*⁶ using a generalized BCS Hamiltonian for the
 424 two-band superconductor proposed a generalized expression
 425 for critical temperature T_c and temperature-dependent pairing
 426 amplitude. As stated earlier, our two-band Hubbard Hamilto-
 427 nian without the interband pairing term is identical to that of
 428 Suhl *et al.* The expression for T_c for the s and l bands (T_c^s and
 429 T_c^l , respectively) can be generalized to

$$1 = |U_m| \int_{-\infty}^{\infty} dE \frac{\langle\langle N_m(E) \rangle\rangle}{2E} \tanh\left(\frac{E}{2k_B T_c^m}\right), \quad (20)$$

430 where $m = s$ or l , while $\langle\langle N_s(E) \rangle\rangle$ and $\langle\langle N_l(E) \rangle\rangle$ are the
 431 s - and l -band configuration averaged density of states in the
 432 normal state at energy E . Setting $U_s = U_l = 3.5$, $U_{sl} = 0$ and

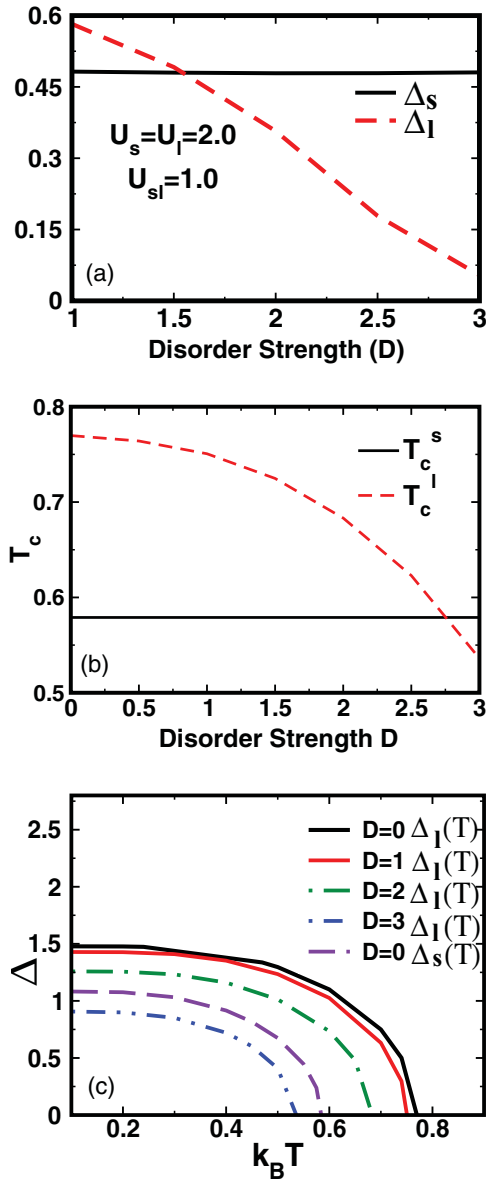


FIG. 4. (Color online) (a) Variation of Δ as a function of disorder strength (D) in the l band when $U_s = U_l > U_{sl}$. (b) Variations of s -band and l -band critical temperatures T_c^s and T_c^l as a function of disorder strength D when only intraband pairing occurs in a two-band s -wave superconductor in a square lattice. (c) Variation of $\Delta_s(T)$ and $\Delta_l(T)$ with T for various strengths of disorder D in the l band.

expressions for the temperature-dependent pairing amplitudes are

$$1 = |U_m| \int_{-\infty}^{\infty} dE \frac{\langle \langle N_m(E) \rangle \rangle}{2(E^2 + \Delta_m^2)^{1/2}} \tanh\left(\frac{(E^2 + \Delta_m^2)^{1/2}}{2k_B T}\right)$$

for the $m = s$ or l bands.

We see that with the increase in disorder strength D in the l band the temperature-dependent pairing amplitude Δ_l reduces much like the zero-temperature pairing amplitude [see Fig. 4(c)]. Since randomness in the l channel does not affect the s band thus $\Delta_s(T)$ is not affected by D so we have plotted $\Delta_s(T)$ vs T only at $D = 0$ [see Fig. 4(c)]. We conclude from Figs. 4(b) and 4(c) that for temperatures below the critical temperatures though disorder (D) suppresses $\Delta(T)$, but does not reduce it to zero.

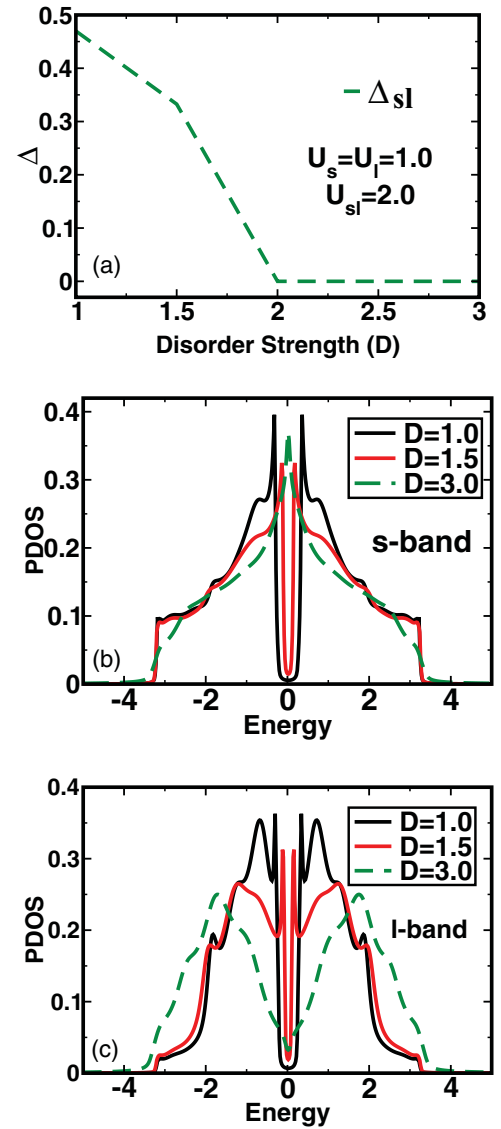


FIG. 5. (Color online) (a) Variation of Δ with disorder strength (D) in the l band when $U_s = U_l < U_{sl}$. (b),(c) Studies DOS for a square-lattice superconducting system with disorder in the l band when $U_s = U_l < U_{sl}$.

433 $x = y = 0.5$ and keeping the system fixed at half filling, we
 434 obtain the corresponding T_c^s and T_c^l for different values of D
 435 [see Fig. 4(b)]. As seen from this figure, T_c^s remains constant
 436 with increasing disorder strength D since randomness in the
 437 l band does not affect the s band in the presence of intraband
 438 pairing alone. T_c^l is, however, suppressed with increasing D . At
 439 this point, however, it must be noted that only the higher of the
 440 two critical temperatures (T_c^s and T_c^l) is physically significant
 441 in this respect. So in the present case, T_c first decreases with
 442 disorder and then becomes constant when $T_c^s > T_c^l$.
 443 These conclusions are further strengthened by a study of
 444 the pairing amplitude as a function of temperature, and the

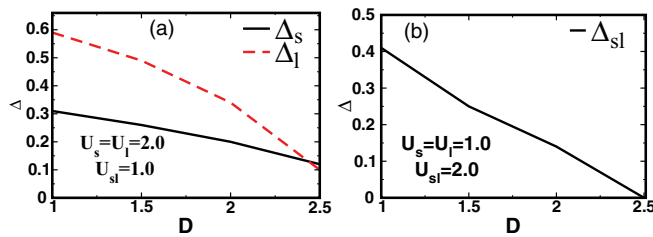


FIG. 6. (Color online) A study of Δ as a function of disorder strength (D) in the s and l band for (a) $U_s = U_l > U_{sl}$ and (b) $U_s = U_l < U_{sl}$ for a two-dimensional (2D) superconducting system having two bands. Here the intraband hopping integrals $t_s = 1.0$ and $t_l = 0.5$ and the interband hopping integral $t_{sl} = 0.0$.

C. Summary

In this paper we have developed a real-space approach to study the effect of disorder on multiband superconductivity using a two-band Hubbard Hamiltonian to model our system and augmented space vector-recursion^{22,23} method to treat randomness in our system. We have established the accuracy of our method by comparing our results in ordered systems with those obtained earlier using other techniques. For ordered systems we have seen gaps in both bands in the presence of intraband pairing. In the presence of both intraband and interband momentum independent pairing, depending on the relative magnitude of the pairing strength, only a particular kind of pairing is possible for a half filled s -like two-band system.

We have then studied the effect of randomness in one of the bands. When only intraband pairing occurs, randomness in one channel does not affect the other. But in the presence of interband pairing both the bands are affected by randomness. By increasing the strength of disorder, superconductivity survives in the presence of intraband pairing although the pairing amplitudes decrease with disorder. However, for interband pairing the gap in the quasiparticle spectrum ceases to exist beyond a critical value of the disorder strength. In the case of interband pairing, where the Cooper pairs are formed by electrons belonging to two different bands, we speculate that phase coherence of the superconducting state is more sensitive to disorder. The lack of phase coherence due to disorder is probably responsible for the disappearance of superconductivity. The same conclusion holds good when disorder is introduced in both the bands. Our calculation indicates that interband pairing in multiband systems is not only interesting but opens up a paradigm beyond Anderson's theorem¹¹ to understand superconductivity in disordered systems.

ACKNOWLEDGMENT

This work was done under the Hydra Collaboration between our groups.

The next set of studies is the investigation of the increasing strength of the disorder D on a two-band attractive- U Hubbard model with dominant interband attractive interaction $U_{sl} > U_s, U_l$. In the parameter regime $U_s = U_l = 1.0 < U_{sl}$ the dominant pairing is the interband pairing U_{sl} and it affects both the bands. In contrast to the case of only intraband pairing, here for a critical strength of disorder $D > 2$ the pairing amplitude Δ_{sl} vanishes indicating the possible disappearance of superconductivity [see Fig. 5(a)]. This is further illustrated in the DOS plot for the s and l channels in Figs. 5(b) and 5(c), respectively. Here the presence of randomness in the l channel affects Δ_{sl} and this in turn affects both s and l PDOS. With increasing disorder D in the l channel the gaps both in the s PDOS and l PDOS reduces. Eventually finite DOS at the Fermi level is realized indicating the absence of superconductivity.

Finally we address the situation when disorder is introduced in both s and l channels. When the interaction is such that $U_s = U_l > U_{sl}$ [Fig. 6(a)], then only Δ_s and Δ_l are nonzero even for strength of disorder as large as $D = 2.5$ indicating the presence of superconductivity. However, in the limit $U_{sl} > U_s = U_l$ [Fig. 6(b)], we see that Δ_{sl} decreases rapidly with disorder and finally vanishes. These features are very similar to the case when disorder was introduced in only one channel.

¹H. J. Choi, D. Roundy, H. Sun, M. L. Cohen, and S. G. Louie, *Nature (London)* **418**, 758 (2002).

²K. I. Wysokinski, G. Litak, J. F. Annett, and B. L. Györfy, *Phys. Status Solidi* **244**, (2007).

³J. F. Annett, G. Litak, B. L. Györfy, and K. I. Wysokinski, *Phys. Rev. B* **66**, 134514 (2002).

⁴M. Daghofer, A. Moreo, J. A. Riera, E. Arrigoni, D. J. Scalapino, and E. Dagotto, *Phys. Rev. Lett.* **101**, 237004 (2008).

⁵S. Raghu, X. L. Qi, C. X. Liu, D. J. Scalapino, and S. C. Zhang, *Phys. Rev. B* **77**, 220503 (2008).

⁶H. Suhl, B. T. Matthias, and L. R. Walker, *Phys. Rev. Lett.* **3**, 552 (1959).

⁷The shape of a band is determined by the diagonal and the hopping matrix elements of the corresponding tight-binding Hamiltonian.

⁸K. Machida, M. Ichioka, M. Takigawa, and N. Nakai (Springer-Verlag, Berlin, 2002), pp. 32–45.

⁹A. Moreo, M. Daghofer, A. Nicholson, and E. Dagotto, *Phys. Rev. B* **80**, 104507 (2009).

¹⁰W. V. Liu and F. Wilczek, *Phys. Rev. Lett.* **90**, 047002 (2003).

¹¹P. W. Anderson, *J. Phys. Chem. Solids* **11**, 26 (1959).

¹²P. G. de Gennes, *Superconductivity in Metals and Alloys* (Benjamin, New York, 1966), p. 140.

¹³R. Moradian, J. F. Annett, B. L. Györfy, and G. Litak, *Phys. Rev. B* **63**, 024501 (2000).

¹⁴A. M. Martin, G. Litak, B. L. Györfy, J. F. Annett, and K. I. Wysokinski, *Phys. Rev. B* **60**, 7523 (1999).

¹⁵G. Litak and B. L. Györfy, *Phys. Rev. B* **62**, 6629 (2000).

¹⁶Shreemoyee Ganguly, A. Venkatasubramanian, Kartick Tarafder, Indra Dasgupta, and Abhijit Mookerjee, *Phys. Rev. B* **79**, 224204 (2009).

¹⁷A. Mookerjee, in *Electronic Structure of Alloys, Surfaces and Clusters*, edited by A. Mookerjee and D. D. Sarma (Taylor & Francis, London, 2003).

- 3 ¹⁸K. I. Wysokinski, G. Litak, J. F. Annett, and B. L. Györfy, *Phys. Status Solidi* **244**, (2007).
- ¹⁹I. Satpathy, D. Goss, and M. K. Banerjee, *Phys. Rev.* **183**, 887 (1969).
- ²⁰A. Mookerjee, *J. Phys. C* **6**, 1340 (1973); **6**, L205 (1973).
- ²¹A. M. Martin and J. F. Annett, *Phys. Rev. B* **57**, 8709 (1998).
- ²²T. J. Godin and R. Haydock, *Phys. Rev. B* **38**, 5237 (1988).
- ²³T. J. Godin and R. Haydock, *Phys. Rev. B* **46**, 1528 (1992).
- ²⁴Y. Wang, T. Plackowski, and A. Junod, *Physica C* **355**, 179 (2001).
- 4 ²⁵H. D. Yang, J. Y. Lin, H. H. Li, F. H. Hsu, C. J. Liu, S. C. Li, R. C. Yu, and C. Q. Jin, *Phys. Rev. Lett.* **87**, 167003 (2001).
- ²⁶H. D. Yang, J. Y. Lin, H. H. Li, F. H. Hsu, C. J. Liu, S. C. Li, R. C. Yu, and C. Q. Jin, *Phys. Rev. Lett.* **87**, 167003 (2001).
- ²⁷P. Szabo, P. Samuely, J. Kacmarcik, T. Klein, J. Marcus, D. Fruchart, S. Miraglia, C. Marcenat, and A. G. M. Jansen, *Phys. Rev. Lett.* **87**, 137005 (2001).
- ²⁸F. Giubileo, D. Roditchev, W. Sacks, R. Lamy, D. X. Thanh, J. Klein, S. Miraglia, D. Fruchart, J. Marcus, and P. Monod, *Phys. Rev. Lett.* **87**, 177008 (2001).
- ²⁹X. K. Chen, M. J. Konstantinovic, J. C. Irwin, D. D. Lawrie, and J. P. Franck, *Phys. Rev. Lett.* **87**, 157002 (2001).
- ³⁰S. Tsuda, T. Yokoya, T. Kiss, Y. Takano, K. Togano, H. Kito, H. Ihara, and S. Shin, *Phys. Rev. Lett.* **87**, 177006 (2001).